Available online at www.sciencedirect.com
ScienceDirect
Biochimica et Biophysica Acta 1767 (2007) 725–731
Biochimica et Biophysica Acta BBA
www.elsevier.com/locate/bbabio

Organisation of Photosystem I and Photosystem II in red alga *Cyanidium caldarium*: Encounter of cyanobacterial and higher plant concepts

Zdenko Gardian [a,b], Ladislav Bumba [a,c], Adam Schrofel [d], Miroslava Herbstova [a,e], Jana Nebesarova [a,e], Frantisek Vacha [a,b,e,*]

[a] *Biological Centre, Academy of Sciences of the Czech Republic, Branišovská 31, 370 05 České Budějovice, Czech Republic*
[b] *Institute of Physical Biology, University of South Bohemia, Zámek 136, 373 33 Nové Hrady, Czech Republic*
[c] *Institute of Microbiology, Academy of Sciences of the Czech Republic, Vídeňská 1083, 142 20 Praha 4, Czech Republic*
[d] *Department of Biochemistry, Faculty of Science, Charles University, Albertov 6, 128 43 Praha 2, Czech Republic*
[e] *Faculty of Biological Sciences, University of South Bohemia, Branišovská 31, 370 05 České Budějovice, Czech Republic*

Received 29 September 2006; received in revised form 19 January 2007; accepted 30 January 2007
Available online 7 February 2007

Abstract

Structure and organisation of Photosystem I and Photosystem II isolated from red alga *Cyanidium caldarium* was determined by electron microscopy and single particle image analysis. The overall structure of Photosystem II was found to be similar to that known from cyanobacteria. The location of additional 20 kDa (PsbQ′) extrinsic protein that forms part of the oxygen evolving complex was suggested to be in the vicinity of cytochrome *c*-550 (PsbV) and the 12 kDa (PsbU) protein. Photosystem I was determined as a monomeric unit consisting of PsaA/B core complex with varying amounts of antenna subunits attached. The number of these subunits was seen to be dependent on the light conditions used during cell cultivation. The role of PsaH and PsaG proteins of Photosystem I in trimerisation and antennae complexes binding is discussed.

Keywords: Photosynthesis; Red algae; *Cyanidium caldarium*; Photosystem I; Photosystem II; Electron microscopy

1. Introduction

Red algae (*Rhodophyta*) are, in evolutionary terms, one of the most primitive eukaryotic algae. The photosynthetic apparatus of red algae appears to represent a transitional state between cyanobacteria and chloroplasts of photosynthetic eukaryotes. The ultrastructure of red algal chloroplasts is similar to that of cyanobacteria, where thylakoid membranes are not differentiated into stacked and unstacked membrane regions as found in chloroplast of higher plants and green algae [1,2]. Both cyanobacteria and the red algae contain phycobilisomes that serve as the primary light-harvesting antenna for Photosystem II (PSII) complex instead of chlorophyll (Chl) *a/b* (or Chl *a/c*)-binding proteins found in higher plants and algae [3,4]. However, the rhodophytes like all major groups of photosynthetic eukaryotes have an intrinsic light-harvesting complex associated with Photosystem I (PSI) [5–7].

PSII contains more than 25 subunits (coded by *psbA-psbZ* genes) and it catalyzes series of photochemical reactions resulting in a reduction of plastoquinone and oxidation of water to molecular oxygen [8,9]. The PSII core complex is apparently highly conserved throughout the photosynthetic organisms and its structure in cyanobacteria has been recently determined by X-ray crystallography [10–12]. However, slight differences can be found on the lumenal side of PSII covered by the extrinsic proteins of the oxygen-evolving complex (OEC) (for recent review see Ref. [13]). Among the extrinsic proteins, only the 33 kDa protein (PsbO) is common to all of the

Abbreviations: Chl, chlorophyll; DEAE, diethyaminoethyl; DM, *n*-dodecyl-β-D-maltoside; EM, electron microscopy; HL, high light; LHCI, light-harvesting complex of Photosystem I; LHCII, light-harvesting complex of Photosystem II; LL, low light; MES, 2-morpholinoethanesulfonic acid; OEC, oxygen evolving complex; PSI, Photosystem I; PSII, Photosystem II; SDS-PAGE, polyacrylamide gel electrophoresis in a presence of sodium dodecylsulfate

* Corresponding author. Biological Centre, Academy of Sciences of the Czech Republic, Branišovská 31, 370 05 České Budějovice, Czech Republic. Tel.: +420 387775533; fax: +420 385310356.
E-mail address: vacha@jcu.cz (F. Vacha).

0005-2728/$ - see front matter © 2007 Elsevier B.V. All rights reserved.
doi:10.1016/j.bbabio.2007.01.021

oxygenic photosynthesis organisms [14]. In addition, higher plants and green algae contain the 23 kDa (PsbP) and 16 kDa (PsbQ) extrinsic proteins. In cyanobacteria and red algae, these proteins are missing and are replaced by cytochrome *c*-550 (PsbV) and 12 kDa protein (PsbU) [15]. In a red alga *Cyanidium caldarium*, a fourth extrinsic protein with a molecular mass of 20 kDa (PsbQ′) has been discovered [16], however, its appearance was recently reported also in other species [17].

PSI is a multisubunit protein complex, which mediates the light-driven electron transport from plastocyanin to ferredoxin, providing the electrons for a reduction of $NADP^+$ [18,19]. PSI contains more than 12 subunits, denoted as PsaA to PsaO, of which the PsaA and PsaB form a heterodimer in the central part of the complex. The structure of the PSI core complex has been resolved in the cyanobacterium *Synechococcus elongatus* [20] and in pea (*Pisum sativum*) [21] to a resolution of 2.5 and 4.4 Å, respectively. In prokaryotes, PSI has been shown to exist *in vivo* predominantly in trimeric form [22,23] as compared to PSI monomers reported for the eukaryotic organisms [24,25].

The peripheral antenna of PSI is fundamentally different in various groups of organisms. In cyanobacteria, phycobilisomes may act as peripheral antenna systems for PSI under normal growth conditions [1], though under iron limitation a membrane-intrinsic protein IsiA (CP43′) replaces phycobilisomes and forms a closed ring of 18 subunits around the trimeric PSI [26]. Oceanic *Prochlorococcus marinus* [27] and freshwater *Prochlothrix hollandica* [28] were also shown to have a ring of 18 subunits of membrane intrinsic Pcb antenna proteins around the trimeric PSI. In higher plants and algae, monomeric PSI is associated with the peripheral light-harvesting antenna complex I (LHCI) made up of nuclear-encoded Lhca proteins [6,7]. The Lhca proteins are highly conserved within all photosynthetic eukaryotes and have a structure similar to that of the related Lhcb proteins of the light-harvesting complex of PSII (LHCII) complex of higher plant PSII [4]. In the red alga *C. caldarium* five chl *a*-binding antenna proteins, ranging in size from about 16 to 23 kDa, have been identified [29,30].

In this work, we investigated the supramolecular organisation of the PSII and PSI complexes isolated from the red alga *C. caldarium* by means of electron microscopy (EM) and single particle image analysis. The analysis of dimeric PSII complex revealed the location of the extrinsic OEC proteins on the lumenal surface of the PSII complex. The image analysis of the PSI–LHCI supercomplex showed PSI as a monomeric particle with LHCI antenna proteins bound along one side of the PSI complex. The influence of light intensities during cell growth on the PSI–LHCI supercomplex organisation was also studied.

2. Materials and methods

The red alga *C. caldarium* was grown in 10 l flasks at 42 °C in a *Cyanidium* medium [31] and bubbled with filtered air. The algal suspension was cultured under low light (LL) or high light (HL) irradiances of 20 or 200 μmol photon m^{-2} s^{-1}, respectively.

Cells were harvested by centrifugation at 1800×*g* for 5 min, washed with distilled water, and resuspended in a buffer A containing 50 mM 2-morpholinoethanesulfonic acid (Mes), pH 6.5, 10 mM NaCl, 5 mM $CaCl_2$ and 20% (v/v) glycerol. The cells were broken with glass beads (100–200 μm) in a Beadbeater cell homogenizer (BioSpec Products, Inc., Bartlesville, OK, USA) for 10 cycles (15 s shaking with 3 min break). The suspension was sieved through a nylon cloth (20 μm) and unbroken cells were removed by centrifugation for 5 min at 3200×*g*. The supernatant was then centrifuged for 1 h at 60,000×*g* to pellet thylakoid membranes. The thylakoid membranes were then washed with buffer A, pelleted, and resuspended for several times to completely remove phycobilisomes.

Thylakoid membranes were resuspended in buffer containing 20 mM Mes (pH 6.5), 10 mM NaCl, 5 mM $CaCl_2$ and solubilised with 1% *n*-dodecyl-β-D-maltoside (DM) at a chlorophyll concentration of 1 mg(Chl) ml^{-1} for 20 min. The unsolubilised material was removed by centrifugation for 20 min at 60,000×*g* and the supernatant was loaded onto a fresh 0–1.2 M continuous sucrose density gradient prepared by freezing and thawing the centrifuge tubes filled with a buffer containing 20 mM Mes (pH 6.5), 0.6 M sucrose, 10 mM NaCl, 5 mM $CaCl_2$, 0.03% DM. The following centrifugation was carried out at 4 °C using a P56ST swinging rotor (Sorvall) at 150,000×*g* for 14 h.

Three colour zones were resolved in the sucrose density gradient. The second green zone containing both PSI and PSII complexes was harvested with a syringe and subjected to a DEAE Sepharose CL-6B (Amersham Biosciences, Sweden) anion-exchange column equilibrated with 50 mM Mes (pH 6.2), 5 mM $CaCl_2$, 0.03% DM. The PSI and PSII complexes were eluted at concentration of 25 mM and 300 mM NaCl, respectively. PSI and PSII complexes isolated by anion-exchange chromatography were further purified and desalted by gel filtration using Sephadex G-25 (Amersham Biosciences, Sweden) [32].

Chlorophyll concentrations were determined according to Ogawa and Vernon [33]. Room temperature absorption spectra were recorded with a UV300 spectrophotometer (Spectronic Unicam, Cambridge, UK). Fluorescent emission spectra were measured at a liquid nitrogen temperature using a Fluorolog-2 spectrofluorometer (Jobin Yvon, Edison, NJ, USA) with an excitation

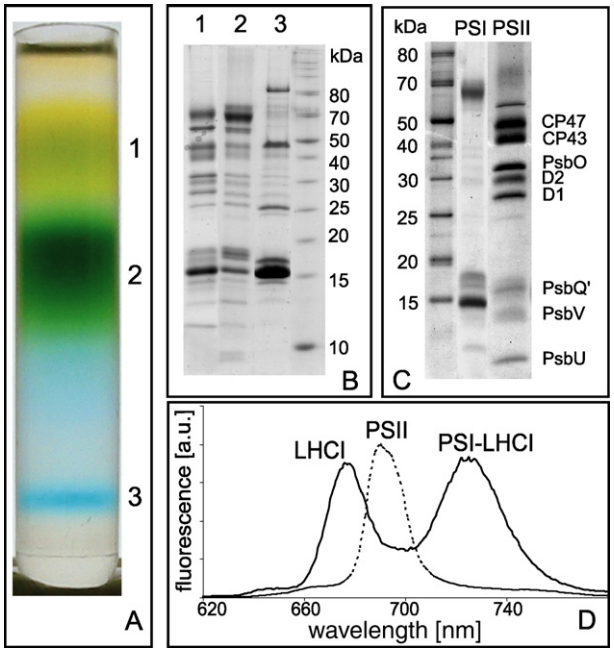

Fig. 1. Isolation and analysis of pigment–protein complexes from thylakoid membranes of *C. caldarium*. (A) Three main zones (1, 2 and 3) were resolved after sucrose density gradient centrifugation of thylakoid membranes from *C. caldarium*. Thylakoid membranes were solubilized with 1% *n*-dodecyl-β-D-maltoside and separated on a linear 0–1.2 M sucrose density gradient. (B) SDS-PAGE analysis of the three sucrose density gradient zones. Lanes 1–3 represent zones 1–3 from the sucrose density gradient. (C) SDS-PAGE analysis of the fractions eluted from DEAE Sepharose CL-6B anion-exchange column. PSI-fraction eluted from the column with 25 mM NaCl. PSII- fraction eluted from the column with 300 mM NaCl. Molecular weight markers (in kDa) are indicated on the left. (D) 77 K fluorescence emission spectra of the PSI (solid line) and PSII (dashed line) fractions eluted from anion-exchange column.

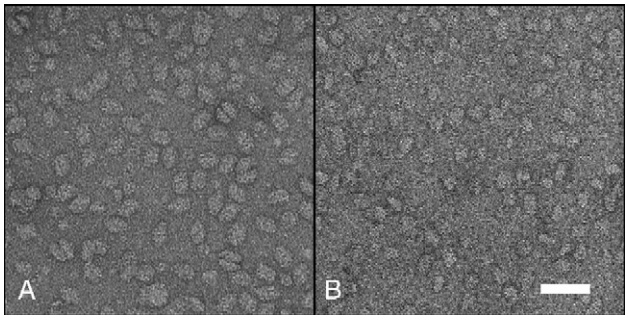

Fig. 2. Electron micrographs of PSII (A) and PSI (B) complexes in their top-view projections. Samples were negatively stained with 2% uranyl acetate. The scale bar represents 50 nm.

wavelength of 435 nm and a chlorophyll concentration of 10 μg (Chl) ml^{-1}. The protein composition was determined by SDS-PAGE using a 12.5% polyacrylamide gel containing 6 M urea and stained with Coomassie Brilliant Blue. The position of PsbV protein was detected in SDS-PAGE gel by a heme staining [32].

For the N-terminal sequencing the proteins were separated by SDS-PAGE and transferred to the PVDF membrane (Hybond, USA) in a Towbin buffer. After the transfer the membrane was washed in distilled water and stained with Coomassie Blue. The corresponding protein band was cut from the membrane and used for N-terminal sequencing. The sequence was determined by using model 491 Procise Protein Sequencing System (Perkin Elmer, Applied Biosystems, USA) based on Edman degradation method.

Freshly prepared PSI and PSII complexes were immediately used for electron microscopy (EM). The specimen was placed on glow-discharged carbon-coated copper grids and negatively stained with 2% uranyl acetate. EM was performed with JEOL 1010 transmission electron microscope (JEOL, Japan) using 80 kV at 60,000× magnification. EM micrographs were digitized with a pixel size corresponding to 5.1 Å at the specimen level. Image analyses were carried out using Spider and Web software package [34]. The selected projections were rotationally and translationally aligned, and treated by multivariate statistical analysis in combination with classification procedure [35,36]. Classes from each of the subsets were used for refinement of alignments and subsequent classifications. For the final sum, the best of the class members were summed using a cross-correlation coefficient of the alignment procedure as a quality parameter.

3. Results and discussion

Three colour zones were resolved on sucrose density gradient after centrifugation of DM solubilised thylakoid membranes (zones 1–3, Fig. 1A). The two upper zones 1 and 2 contained mainly green chlorophyll–protein complexes, while the third blue zone contained the detached phycobilisomes. SDS-PAGE analysis (Fig. 1B) showed that the zone 2 was enriched with PSI and PSII complexes. It should be pointed out that we did not observe any differences in the sucrose density gradient zone patterns as well as in protein composition between thylakoid membranes from HL and LL cultures.

3.1. Photosystem II

PSII complexes from *C. caldarium* were isolated from the zone 2 of the sucrose density gradient centrifugation followed with the anion-exchange chromatography. As shown in Fig. 1C, the PSII fraction contained major PSII subunits (CP47, CP43, D2 and D1), as well as four extrinsic proteins of the oxygen-evolving complex typical for red algal preparation (PsbO, PsbV, PsbQ′ and PsbU). The presence of PsbV in the PSII complex was confirmed by heme staining of the SDS-PAGE gel (data not shown). The identity of the recently discovered PsbQ′ protein was confirmed by N-terminal sequencing. The N-terminal analysis of the PsbQ′ protein band led to a sequence of 12 amino acids which is identical with a position between 73 and 84 amino acid residues of psbQ-like protein [37]. The position of these 12 amino acids suggests that the first 72 amino acids of the PsbQ′ protein precursor serves as a target sequence for protein transport from cytosol to chloroplast thylakoid membrane. Room temperature absorption spectrum of the PSII complex lacked the significant absorbance around 623 nm indicating that the sample was free of phycobiliproteins (spectrum not shown). The fluorescence emission spectrum of PSII fraction had one

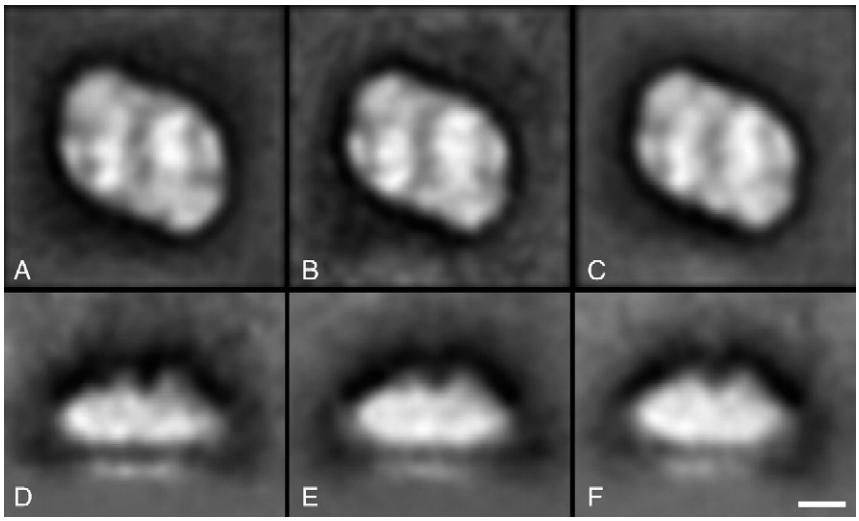

Fig. 3. Single particle analysis of top-view and side-view projection maps of *C. caldarium* PSII complexes. (A–C) The three most representative class averages obtained by classification of 5840 top-view projections. The projections are presented as facing from the lumenal side of the complex. (D–F) The three most representative class averages obtained by classification of 4500 side-view projections. The average images represent PSII complexes in their side-view projections. Proteins of the oxygen-evolving complex are visualized as protrusions on the lumenal surface of the PSII complex. The number of summed images is: 685 (A), 715 (B), 695 (C), 650 (D), 462 (E) and 576 (F). The scale bar represents 5 nm.

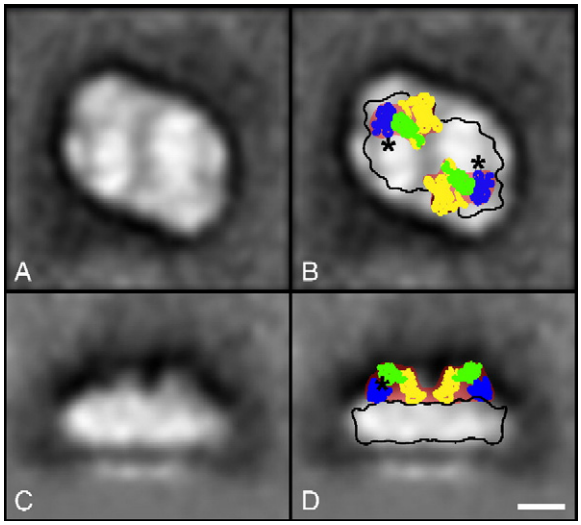

Fig. 4. Schematic representation of subunit organisation of the extrinsic subunits on the lumenal side of dimeric PS II in the red alga *C. caldarium*. The most representative top-view (A) and side-view (C) projection maps of negatively stained PSII core complex from *C. caldarium*. The corresponding top-view (B) and side-view (D) projections overlaid with a cyanobacterial X-ray model of the PSII complex. Red areas indicate the locations of extrinsic subunits. The coordinates are taken from Protein Data Bank (http://www.rcsb.org/pdb), code 1S5L [11] and 2AXT [12]. The Cα backbone of the PsbO (yellow), PsbV (blue) and the PsbU subunits (green) are illustrated. For clarity the underlying transmembrane helices are not demonstrated. The proposed location of the red algal PsbQ' extrinsic subunit is indicated by a black star. Bar represents 5 nm.

characteristic peak emitting at 690 nm with a shoulder at 695 nm. For electron microscopy (EM) the PSII complex was further purified using a gel filtration chromatography.

The dimeric PSII complexes were immobilized on glow-discharged carbon-coated EM grid, negatively stained with uranyl acetate and visualized in transmission electron microscope (Fig. 2A). The EM images contained dimeric PSII particles, mostly in their top-view projections (i.e. perpendicular to the original membrane plane). Side-view projections were less common and usually occurred as an aggregation of two single PSII complexes attached to each other by their stromal surfaces [38,39].

To process the particle images by single particle analysis, a large data set was extracted from the images and the projections were aligned, treated with multivariate statistical analysis and classified into classes. A total of 5840 top-view projections were selected for analysis. After the classification step the top-view data set was decomposed into eight classes, three of which are presented in Fig. 3A–C. The top-view projections show diamond-shaped particles with two-fold rotational symmetry around the centre of the complex. The class averages were similar in size and shape, and they closely resemble the PSII core complexes isolated from cyanobacteria, algae and higher plants [31,38–41]. All the projections had the same type of handedness and no mirror images were detected, thus indicating a preferred orientation of the PSII dimers with their stromal side to the carbon support film.

Side-view projections were characterised as an aggregate of two neighbouring PSII particles. For image analysis we have selected 4500 single side-view particles out of 2350 projections of side-view aggregates. The classification of such images resulted in the set of eight classes and the most representative class averages are depicted in Fig. 3D–F. The side-view projections slightly differed between each other with respect to the overall length of the particle, which represented projections of particles that are not attached with the longest axis parallel to the carbon support film [40]. The most abundant class average (Fig. 4) showed two separated protrusions, symmetrically located with respect to the centre of the complex. The inner protrusions have been previously identified as the PsbO extrinsic

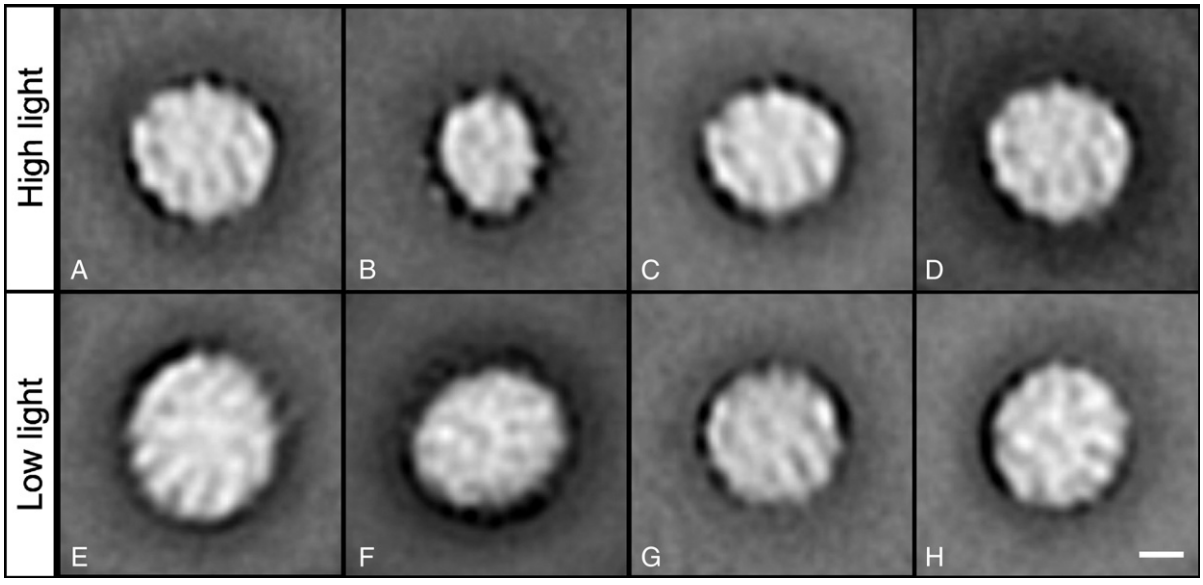

Fig. 5. Single particle analysis of top-view projection maps of *C. caldarium* PSI complexes. (A–D) The most representative class averages obtained by classification of 7740 particles from the high light (HL) culture. (E–H) The most representative class averages obtained by classification of 11000 particles from the low light (LL) culture. The scale bar represents 5 nm. The number of averaged particles is 715 for A, 810 for B, 664 for C, 414 for D, 817 for E, 907 for F, 450 for G and 912 for H.

subunit, while the outer protrusions were occupied by the PsbV and PsbU subunits [13,40].

In the red alga *C. caldarium*, the fourth additional extrinsic protein, PsbQ′, has been reported by Enami and co-workers [16]. In later study, the authors proposed that this extrinsic protein is not involved directly in oxygen evolution [42]. Since we have identified the presence of the PsbQ′ subunit in our PSII preparation, we also tried to identify the location of this protein within the PSII dimer. A comparison between the projection maps of the top and side-view projections from *C. caldarium* (Fig. 4), and those from the red alga *Porphyridium cruentum* [32] and cyanobacterium *S. elongatus* [40], did not reveal any additional protein densities that could be assigned to the PsbQ′ protein.

We assume that in our side-view projection the PsbO, PsbV and the PsbU protein densities of OEC are eclipsing the PsbQ′ protein and, therefore, a protein density corresponding to the PsbQ′ subunit could not be assigned. Since the more probable place close to the PsbO and PsbU protein is occupied by the external loop of CP47 protein [10–12] we have suggested a putative location of the PsbQ′ protein in a close vicinity of PsbV and the PsbU subunits (black star in Fig. 4). This model well corresponds with conclusions of Enami et al. [42] who proposed the role of PsbQ′ as a mediator in proper binding of PsbV and PsbU proteins in OEC complex.

3.2. Photosystem I

PSI complexes from both HL and LL cultures were isolated from the second zone of the sucrose density gradient centrifugation followed with anion-exchange chromatography. SDS-PAGE analysis of PSI fraction is shown in Fig. 1C. PSI preparations were characterized by an intensive band around 60 kDa corresponding to the PsaA/B reaction centre proteins with few bands around 15 kDa corresponding to LHCI proteins and small PSI subunits. 77 K fluorescence emission spectra of PSI preparation exhibited peak at 725 nm, a typical region of fluorescence emission of PSI, and second peak at 677 nm due to the emission of LHCI complex.

Fig. 2B shows negatively stained PSI complexes in their top-view projections. We have selected about 7740 particles for the analysis of PSI complexes isolated from the HL culture and 11000 particles from the LL culture. After single particle analysis PSI complexes were divided into ten and twelve classes for HL and LL cultures, respectively. The averaged top-view projections of all classes had an oval shape with no apparent symmetry. The class averages represent monomeric PSI particles with very uneven stain distribution at the edge of most of the complexes, as shown previously in green algae and higher plants [24,25]. Three main different sizes of particles were observed. Small particle with a size of 10×14 nm was present in HL cultivation only. Middle size nearly-circular particles with a radius of 16 nm were observed in both HL and LL cultivation and large 16×19 nm oval particle in LL cultivation only. Fig. 5 illustrates variations in size and shape of different class averages of each HL and LL cultures.

The position of the PSI complex within the analysed particles can be deduced from the density variations. The most representative class averages of HL and LL cultivations with overlaid PSI structures are shown in Fig. 6. The small particle from HL cultivation (Fig. 6A) can be overlaid with a PSI core complex (PsaA/B heterodimer) obtained from the higher plants X-ray structure [21], determining the particle as a monomeric PSI core complex (Fig. 6E). Two classes of the middle size PSI particles (Fig. 6B and C), each originated in HL or LL cultures can be overlaid with a projection of X-ray structure of plant PSI–LHCI supercomplex containing PsaA/B heterodimer and a row

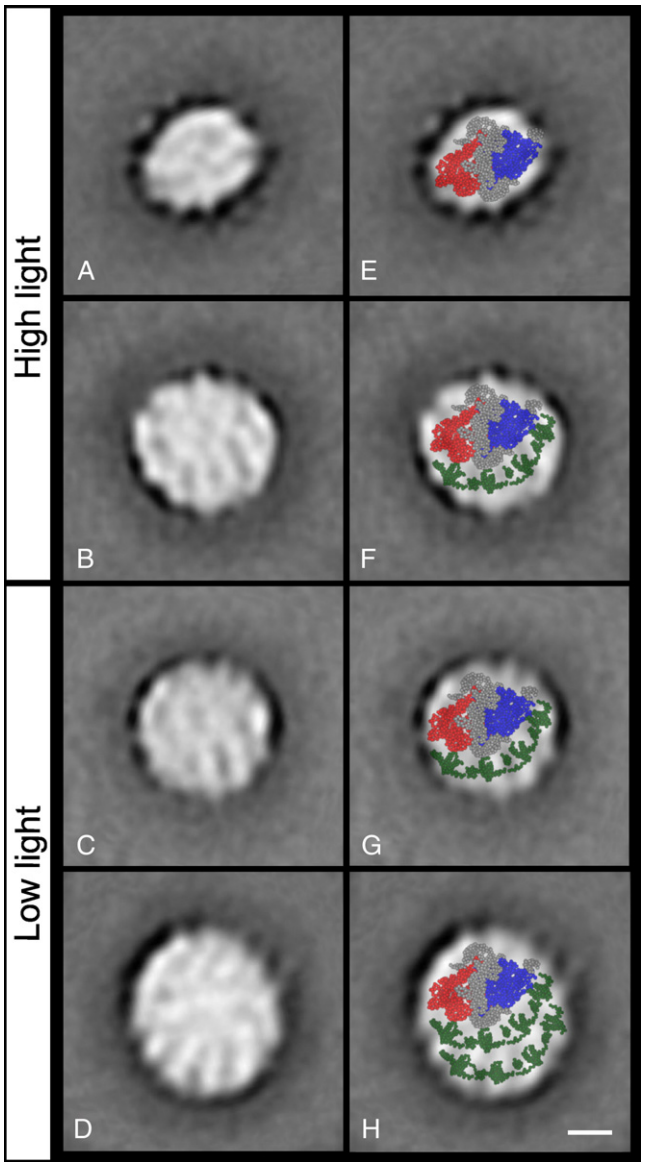

Fig. 6. Schematic representation of the LHCI subunits organisation in PSI complexes isolated from *C. caldarium*. (A, B, E, F) Analysis of PSI particles from the HL cultivation and (C, D, G, H) from the LL cultivation, respectively. Left column represents the most representative class averages of top-view PSI projections. In the right column, these projections are overlaid with PSI core or PSI–LHCI supercomplexes having different number of LHCI subunits. The coordinates were used from the X-ray structure of PSI complex of higher plants (*P. sativum*), Protein Data Bank (http://www.rcsb.org/pdb), code 1QZV [20]. Blue colour in the overlaid structure represents PsaA subunit, PsaB protein is in red and LHCI subunits are in green. The rest of the PSI subunits are in grey colour. The scale bar represents 5 nm.

of four LHCI subunits [21]. The overlaid structure can be adjusted into its position by masking the protrusions on one side of the particle with LHCI subunits (Fig. 6F and G). The class average of the largest PSI particles is shown in Fig. 6D. The overlay of this class average with the plant PSI–LHCI supercomplex shows that there are additional protein densities. We assign the majority of this density to the second row of LHCI protein subunits (Fig. 6H). From these results we conclude that the red alga *C. caldarium* can adapt to different light regimes by changing the effective size of PSI antennae.

The image analysis of PSI complexes from *C. caldarium* did not reveal any other types of particles, such as dimeric or trimeric association of PSI particles as found in cyanobacteria [23]. The size and shape of our particles are very similar to the PSI core or PSI–LHCI supercomplexes observed previously in higher plants [24] or *Chlamydomonas reinhardtii* [25,43].

The presence of the PsaL subunit was suggested to be essential for the trimeric association of PSI [44,45], which is unique for cyanobacteria. However, it was shown that, in *Synechocystis* phosphatidylglycerole-minus mutants, the presence of PsaL subunit in the PSI is not sufficient for the trimerisation if the cells are depleted of phosphatidylglycerole [46]. By superimposing the plant PSI monomers on top of the cyanobacterial trimer, Ben-Shem et al. [47] concluded that plant PSI complexes cannot form trimers because their PsaH subunit, not present in cyanobacteria, completely hinders the contact site of PsaL subunits among the monomers. As the PsaH subunit probably forms part of the docking site for LHCII they imply that trimerisation was lost in plants to facilitate re-allocation of phosphorylated LHCII to PSI under light conditions favouring PSII excitation [21]. Alike in cyanobacteria, PsaH subunit is missing also in red algae [48,49]. Since, in our work, we have observed only PSI monomers, we suggest that the trimerisation is not caused by a simple absence of PsaH subunit in PSI complex.

Another important difference in the protein composition of PSI complex among higher plants, red algae and cyanobacteria is the absence of PsaG protein in cyanobacteria and rhodophytes [48,49]. PsaG subunit was proposed to serve as an anchor site for LHCI binding, forming a helix bundle with Lhca1 and contributing to the intramembrane interaction between the core and the antenna belt [47]. By contrast, we were able to see one or two rows of LHCI antennae complexes attached to the PSI of red alga *C. caldarium* where the PsaG subunit is missing. On the basis of our results, we assume that the presence of PsaG protein is not essential for binding of LHCI subunits and formation of antennae rows in PSI complexes.

In this paper we have demonstrated that red algae are on the edge between cyanobacteria and higher plant evolution path retaining the PSII complex of the cyanobacterial type, however, with the PSI complex already evolved in the higher plant type structure.

Acknowledgments

Authors would like to thank Dr. Zdenek Voburek from the Institute of Organic Chemistry and Biochemistry, Academy of Sciences of the Czech Republic for the N-terminal sequencing. The work was supported by grants MSMT MSM6007665808, AV0Z50510513, GAAV A608170603, GACR 310/07/P115 and GACR 206/06/0364. Authors would like to thank Frantisek Matousek and Ivana Hunalova for technical assistance.

References

[1] E. Gantt, Supramolecular membrane organization, in: D.A. Bryant (Ed.), The Molecular Biology of Cyanobacteria, Kluwer Academic Publishers, Dordrecht, 1994, pp. 139–216.
[2] L. Mustardy, G. Garab, Granum revisited. A three-dimensional model—Where things fall into place, Trends Plant Sci. 8 (2003) 117–122.
[3] E. Mörschel, The light-harvesting antennae of cyanobacteria and red algae, Photosynthetica 25 (1991) 137–144.
[4] B.R. Green, D.G. Durnford, The chlorophyll-carotenoid proteins of oxygenic photosynthesis, Annu. Rev. Plant Physiol. Plant Mol. Biol. 47 (1996) 685–714.
[5] G.R. Wolfe, F.X. Cunningham Jr., D. Durnford, B.R. Green, E. Gantt, Evidence for a common origin of chloroplasts with light-harvesting complexes of different pigmentation, Nature 367 (1994) 566–568.
[6] S. Jansson, The light-harvesting chlorophyll a/b binding-proteins, Biochim. Biophys. Acta 1184 (1994) 1–19.
[7] H.V. Scheller, P.E. Jensen, A. Haldrup, C. Lunde, J. Knoetzel, Role of subunits in eukaryotic Photosystem I, Biochim. Biophys. Acta 1507 (2001) 41–60.
[8] O. Hansson, T. Wydrzynski, Current perceptions of photosystem II, Photosynth. Res. 23 (1990) 131–162.
[9] J. Barber, J. Nield, E.P. Morris, D. Zheleva, B. Hankamer, The structure, function and dynamics of photosystem II, Physiol. Plant. 100 (1997) 817–827.
[10] N. Kamiya, J.R. Shen, Crystal structure of oxygen-evolving photosystem II from *Thermosynechococcus vulcanus* at 3.7-Å resolution, Proc. Nat. Acad. Sci. U. S. A. 100 (2003) 98–103.
[11] K.N. Ferreira, T.M. Iverson, K. Maghlaoui, J. Barber, S. Iwata, Architecture of the photosynthetic oxygen-evolving center, Science 303 (2004) 1831–1838.
[12] B. Loll, J. Kern, W. Saenger, A. Zouni, J. Biesiadka, Towards complete cofactor arrangement in the 3.0 Å resolution structure of photosystem II, Nature 438 (2005) 1040–1044.
[13] L. Bumba, F. Vacha, Electron microscopy in structural studies of photosystem, Photosynth. Res. 77 (2003) 1–19.
[14] A. Seidler, The extrinsic polypeptides of photosystem II, Biochim. Biophys. Acta 1277 (1996) 35–60.
[15] J.R. Shen, M. Ikeuchi, Y. Inoue, Stoichiometric association of extrinsic cytochrome *c*550 and 12-kDa protein with a highly purified oxygen-evolving photosystem II core complexes from *Synechococcus vulcanus*, FEBS Lett. 301 (1992) 145–149.
[16] I. Enami, H. Murayama, H. Ohta, M. Kamo, K. Nakazato, J.R. Shen, Isolation and characterization of a photosystem II complex from the red alga *Cyanidium caldarium*: association of cytochrome *c*550 and a 12(kDa protein with the complex, Biochim. Biophys. Acta 1232 (1995) 208–216.
[17] I. Enami, T. Suzuki, O. Tada, Y. Nakada, K. Nakamura, A. Tohri, H. Ohta, I. Inoue, J.-R. Shen, Distribution of the extrinsic proteins as a potential marker for the evolution of photosynthetic oxygen-evolving photosystem II, FEBS J. 272 (2005) 5020–5030.
[18] P.R. Chitnis, Photosystem I: function and physiology, Annu. Rev. Plant Physiol. Plant Mol. Biol. 52 (2001) 593–626.
[19] P. Fromme, P. Jordan, N. Krauss, Structure of photosystem I, Biochim. Biophys. Acta 1507 (2001) 5–31.
[20] P. Jordan, P. Fromme, H.T. Witt, O. Klukas, W. Saenger, N. Krauss, Three-dimensional structure of cyanobacterial photosystem I at 2.5 Å resolution, Nature 411 (2001) 909–917.
[21] A. Ben-Shem, F. Frolow, N. Nelson, Crystal structure of plant photosystem I, Nature 426 (2003) 630–635.
[22] G.W.M. van der Staay, E.J. Boekema, J.P. Dekker, C.P. Matthijs, Characterization of trimeric Photosystem I particles from the prochlorophyte

Prochlorothrix hollandica by electron microscopy and image analysis, Biochim. Biophys. Acta 1142 (1993) 189–193.

[23] J. Kruip, P.R. Chitnis, B. Lagoutte, M. Rogner, E.J. Boekema, Structural organization of the major subunits in cyanobacterial photosystem I. Localization of subunits PsaC, -D, -E, -F, and -J, J. Biol. Chem. 272 (1997) 17061–17069.

[24] E.J. Boekema, P.E. Jensen, E. Schlodder, J.F.L. van Breemen, H. van Roon, V.H. Scheller, J.P. Dekker, Green plant photosystem I binds light-harvesting complex I on one side of the complex, Biochemistry 40 (2001) 1029–1036.

[25] M. Germano, A.E. Yakushevska, W. Keegstra, H.J. van Gorkom, J.P. Dekker, E.J. Boekema, Supramolecular organization of photosystem I and light-harvesting complex I in *Chlamydomonas reinhardtii*, FEBS Lett. 525 (2002) 121–125.

[26] T.S. Bibby, J. Nield, J. Barber, Three-dimensional model and characterization of the iron stress-induced CP43′-photosystem I supercomplex isolated from the cyanobacterium Synechocystis PCC 6803, J. Biol. Chem. 276 (2001) 43246–43252.

[27] T.S. Bibby, I. Mary, J. Nield, F. Partensky, J. Barber, Low-light-adapted *Prochlorococcus* species possess specific antennae for each photosystem, Nature 424 (2003) 1051–1054.

[28] L. Bumba, O. Prasil, F. Vacha, Antenna ring around trimeric photosystem I in chlorophyll b containing cyanobacterium *Prochlorothrix hollandica*, Biochim. Biophys. Acta 1708 (2005) 1–5.

[29] J. Marquardt, S. Wans, E. Rhiel, A. Randolf, W.E. Krumbein, Intron–exon structure and gene copy number of a gene encoding for a membrane-intrinsic light-harvesting polypeptide of the red alga *Galdieria sulphuraria*, Gene 255 (2000) 257–265.

[30] J. Marquardt, B. Lutz, S. Wans, E. Rhiel, W.E. Krumbein, The gene family coding for the light-harvesting polypeptides of photosystem I of the red alga *Galdieria sulphuraria*, Photosynth. Res. 68 (2001) 121–130.

[31] M.B. Allen, Studies with *Cyanidium caldarium*, an anomalously pigmented chlorophyte, Arch. Mikrobiol. 32 (1959) 270–277.

[32] L. Bumba, H. Havelkova-Dousova, M. Husak, F. Vacha, Structural characterization of photosystem II complex from red alga *Porphyridium cruentum* retaining extrinsic subunits of the oxygen-evolving complex, Eur. J. Biochem. 271 (2004) 2967–2975.

[33] T. Ogawa, L.P. Vernon, Increased content of cytochromes 554 and 562 in *Anabaena variabilis* cells grown in the presence of diphenylamine, Biochim. Biophys. Acta 226 (1971) 88–97.

[34] J. Frank, M. Radermacher, P. Penczek, J. Zhu, Y.H. Li, M. Ladjadj, A. Leith, SPIDER and WEB: processing and visualization of images in 3D electron microscopy and related fields, J. Struct. Biol. 116 (1996) 190–199.

[35] M. Van Heel, J. Frank, Use of multivariate statistics in analyzing the images of biological macromolecules, Ultramicroscopy 6 (1981) 187–194.

[36] G. Harauz, E.J. Boekema, M. van Heel, Statistical image analysis of electron micrographs of ribosomal subunits, Methods Enzymol. 164 (1988) 35–49.

[37] H. Ohta, T. Suzuki, M. Ueno, A. Okumura, S. Yoshihara, J.R. Shen, I. Enami, Extrinsic proteins of photosystem II: an intermediate member of PsbQ protein family in red algal PS II, Eur. J. Biochem. 270 (2003) 4156–4163.

[38] E.J. Boekema, B. Hankamer, D. Bald, J. Kruip, J. Nield, A.F. Boonstra, J. Barber, M. Rogner, Supramolecular structure of the photosystem II complex from green plants and cyanobacteria, Proc. Natl. Acad. Sci. U. S. A. 92 (1995) 175–179.

[39] L. Bumba, M. Hušák, F. Vácha, Interaction of PSII–LHCII super-complexes in adjacent layers of stacked chloroplast thylakoid membranes, Photosynthetica 42 (2004) 193–199.

[40] H. Kuhl, M. Rogner, J.F. van Breemen, E.J. Boekema, Localization of cyanobacterial photosystem II donor-side subunits by electron microscopy and the supramolecular organization of photosystem II in the thylakoid membrane, Eur. J. Biochem. 266 (1999) 453–459.

[41] F. Vacha, L. Bumba, D. Kaftan, M. Vacha, Microscopy and single molecule detection in photosynthesis, Micron 36 (2005) 483–502.

[42] I. Enami, S. Kikuchi, T. Fukuda, H. Ohta, J.-R. Shen, Binding and functional properties of four extrinsic proteins of photosystem from a red alga, *Cyanidium caldarium*, as studied by release- reconstitution experiments, Biochemistry 37 (1998) 2787–2793.

[43] J. Kargul, J. Nield, J. Barber, Three-dimensional reconstruction of a light-harvesting complex I—Photosystem I (LHCI-PSI) supercomplex from the green alga *Chlamydomonas reinhardtii*, J. Biol. Chem. 278 (2003) 16135–16141.

[44] V.P. Chitnis, P.R. Chitnis, PsaL subunit is required for the formation of photosystem I trimers in the cyanobacterium Synechocystis sp. PCC 6803, FEBS Lett. 336 (1993) 330–334.

[45] R. Kouřil, N. Yeremenko, S. D'Haene, G.T. Oostergetel, H.C.P. Matthijs, J.P. Dekker, E.J. Boekema, Supercomplexes of IsiA and photosystem I in a mutant lacking subunit PsaL, Biochim. Biophys. Acta 1706 (2005) 262–266.

[46] I. Domonkos, P. Malec, A. Sallai, L. Kovács, K. Itoh, G. Shen, B. Ughy, B. Bogos, I. Sakurai, M. Kis, K. Strzalka, H. Wada, S. Itoh, T. Farkas, Z. Gombos, Phosphatidylglycerol is essential for oligomerization of photosystem I reaction center, Plant Physiol. 134 (2004) 1471–1478.

[47] A. Ben-Shem, F. Frolow, N. Nelson, Evolution of photosystem I—From symmetry through pseudosymmetry to asymmetry, FEBS Lett. 564 (2004) 274–280.

[48] H.V. Scheller, P.E. Jensen, A. Haldrup, C. Lunde, J. Knoetzel, Role of subunits in eukaryotic photosystem I, Biochim. Biophys. Acta 1507 (2001) 41–60.

[49] M. Matsuzaki, O. Misumi, T. Shin-i, S. Maruyama, M. Takahara, S. Miyagishima, T. Mori, K. Nishida, F. Yagisawa, K. Nishida, Y. Yoshida, Y. Nishimura, S. Nakao, T. Kobayashi, Y. Momoyama, T. Higashiyama, A. Minoda, M. Sano, H. Nomoto, K. Oishi, H. Hayashi, F. Ohta, S. Nishizaka, S. Haga, S. Miura, T. Morishita, Y. Kabeya, K. Terasawa, Y. Suzuki, Y. Ishii, S. Asakawa, H. Takano, N. Ohta, H. Kuroiwa, K. Tanaka, N. Shimizu, S. Sugano, N. Sato, H. Nozaki, N. Ogasawara, Y. Kohara, T. Kuroiwa, Genome sequence of the ultrasmall unicellular red alga *Cyanidioschyzon merolae* 10D, Nature 428 (2004) 653–657.